

# 1 Kinetics of rapid covalent bond formation of aniline with 2 humic acid: ESR investigations with nitroxide spin labels

3 *Michael Matthies<sup>1\*</sup>, Kevin Glinka<sup>2</sup>, Marius Theiling<sup>2</sup>, Kalman Hideg<sup>3</sup>, Heinz-Jürgen Steinhoff<sup>2</sup>*

4 <sup>1</sup>Institute of Environmental Systems Research (USF), University of Osnabrück, 49069  
5 Osnabrück, Germany

6 <sup>2</sup>Physics Department, University of Osnabrück, 49069 Osnabrück, Germany

7 <sup>3</sup>Department of Organic and Medicinal Chemistry, University of Pécs, [Szigeti st. 12, 7624 Pécs](#),  
8 Hungary

9

10

## 11 **ABSTRACT**

12 The bioavailability of many soil contaminants depends on their interaction with the soil organic  
13 matter. The paper presents a new approach of using stable paramagnetic spin labels for  
14 investigating the kinetics of covalent binding of specific xenobiotic functional groups with humic  
15 acids, a major organic matter fraction. Leonardite humic acid (LHA) was incubated with the  
16 nitroxide spin labels amino-TEMPO (4-amino-2,2,6,6-Tetramethylpiperidin-1-oxyl) and anilino-  
17 NO (2,5,5-Trimethyl-2-(3-aminophenyl)pyrrolidin-1-oxyl), respectively, which contain an  
18 aliphatic or aromatic functionality susceptible to interaction with LHA. Electron spin resonance

19 (ESR) spectra of LHA samples without and with the enzyme laccase were recorded at X-band  
20 frequency (9.43 GHz) at room temperature and neutral pH. Binding was detected by a  
21 pronounced broadening of the spectral lines after incubation of LHA for both spin labels. The  
22 development of a broad signal component in the spectrum of anilino-NO indicated the  
23 immobilization due to strong binding of the aniline group. The reorientational correlation time of  
24 bound anilino-NO is more than two orders of magnitude greater than that of the free label. The  
25 ratio of the amount of bound to the unbound species was used to determine the kinetics of the  
26 covalent bond formation. Reaction rate constants of  $0.16 \text{ min}^{-1}$  and  $0.01 \text{ min}^{-1}$  were determined  
27 corresponding to half-times of 4.3 min and 69.3 min, respectively. Treatment of LHA with  
28 laccase enhanced the amount of the reacting anilino-NO species by a factor of 7.6, but left the  
29 reaction rate unaltered. Oxidative radical coupling was excluded by using the spin trap agent n-  
30 tert-butyl-alpha-phenylnitron.

31 **Keywords:**

32 ESR; spin labeling; nitroxide radical; organic xenobiotics; humic acid; covalent binding; bound  
33 residues; aromatic amines

## 34 INTRODUCTION

35 Human activities, e.g., waste deposition, mining, fertilizing with manure, or application of  
36 chemicals for pest and weed control, have led to contamination of soil systems. Many of these  
37 anthropogenic compounds are synthetic organic chemicals, to which soil has never been  
38 naturally exposed and which are thus called xenobiotics. In biodegradation simulation studies,  
39 many xenobiotic chemicals exhibit a large fraction of residues, which cannot be further extracted  
40 even by harsh methods (non-extractable residues, NER) [1]. Various interaction processes in soil  
41 such as sorption, sequestration (entrapment) or immobilization via binding to soil organic matter  
42 (SOM), clay minerals, and organo-clay complexes [2] govern the extractability and thus their  
43 availability for leaching to groundwater, volatilization, abiotic and biotic degradation, or uptake  
44 by living organisms. NER, also called “bound” residues, have been extensively reviewed, in  
45 particular for pesticides but also for many other organic chemicals [3, 4, 5].

46 Covalent binding of xenobiotics and its metabolites to soil components is of particular interest  
47 because it ultimately withdraws the xenobiotic and its metabolites from any adverse  
48 environmental effect. It is known since many years that functional groups of xenobiotics such as  
49 aromatic amino groups are involved in covalent binding to SOM, in particular to humic  
50 substances (HAs) [6, 7]. Aromatic amines, e.g. aniline (aminobenzene), are the building blocks  
51 of many pesticides, veterinary pharmaceuticals, textile dyes and other classes of synthetic  
52 chemicals and comprise an important class of environmental contaminants [8]. They are also  
53 reductive transformation products of nitro-aromatic explosives such as 2,4,6-trinitrotoluene  
54 (TNT) and received a great deal of attention in remediation of contaminated manufacturing sites  
55 [9 – 11].

56 <sup>15</sup>N NMR studies with aniline and other aromatic amines have revealed nucleophilic addition of  
57 the aromatic amino group to quinone and other carbonyl groups of humic substances [6, 8, 11 -  
58 14]. A fast, reversible 1,2-nucleophilic addition and a slower irreversible 1,4-nucleophilic  
59 addition of the aromatic amino group to the carbonyl group of quinones have been proposed  
60 resulting in the formation of Schiff base (iminoquinone) and Michael amine-carbonyl adducts  
61 (anilinoquinone), respectively. Reaction kinetics of aromatic amines with humic substances has  
62 been studied using ultrafiltration techniques and HPLC for analytic determination [12, 15]. Fast  
63 and slow reaction rate constants were observed in the order of 10<sup>-2</sup> and 10<sup>-3</sup> h<sup>-1</sup>, i.e. half-times of  
64 50 and 500 h, respectively, depending on pH, substitution of the aniline ring, initial aniline  
65 concentration and humic substance [8, 15]. Rapid initial sorption could also be dominated by  
66 irreversibly covalent binding. However, the method applied did not allow determining very fast  
67 reaction kinetics in the first few hours after incubation. Oxidative reaction mechanisms resulting  
68 in the formation of aniline radicals, which couple with radical species, have also been proposed  
69 [16]. Thorn et al. [13] pointed out that radical reactions involving aniline radicals and  
70 semiquinone radicals are possible in the presence of peroxidase or Mn-oxides, as these govern  
71 one-electron oxidation initiated polymerization reactions of aromatic amines and of quinones,  
72 but an open question remained, whether a large pool of quinones is available in soil readily able  
73 to add such a weak nucleophile.

74 The extractability of sulfonamides, which contain an aniline functional group as part of its  
75 antimicrobial active moiety, decreased rapidly in soil incubation studies, even if harsh extraction  
76 methods were applied [17 – 19]. The strong sorption behavior is attributed to the formation of  
77 non-extractable residues (NER). Bialk et al. [20, 21] concluded that the rapid NER formation of  
78 sulfonamides in soil may be due to Michael adducts (anilinoquinones) and Schiff base formation

79 (iminoquinones) of the aromatic amino group, which can only partially be cleaved during  
80 fractionation and vigorous extraction procedures. Bialk and Pedersen [22] observed fungal  
81 peroxidase-mediated covalent coupling of sulfonamide with HA. Gulkowska et al. [23]  
82 proposed a two-step process with an initial formation of imine and anilinoquinone followed by  
83 incorporation into the soil polymer structure. They ruled out oxidative radical coupling with  
84 constituents of SOM as an alternative reaction pathway.

85 ESR spin labeling with stable nitroxide spin labels has successfully been applied since many  
86 years for investigating the structure and dynamics of biological macromolecules and assemblies,  
87 particularly membranes and proteins [24, 25]. Stable nitroxide radicals can also be used for  
88 studying the interaction of xenobiotics in soil and sediment systems. The signal of the  
89 paramagnetic NO group is influenced by its soil microenvironment and can be recorded by ESR  
90 spectroscopy. Using ESR of spin-labelled organic macromolecules such as polysaccharides,  
91 Steen et al. [26] could monitor the sorption to natural sediment surfaces. Sorption specificity and  
92 sorption mechanisms to SOM have been studied by Latta et al. [27] with paramagnetic probes,  
93 where nitroxide compounds of different polarity were used as relaxation agents for NMR  
94 spectroscopy. By means of spin relaxation they could show that nitroxide spin labels exhibit  
95 “little or no preferential sorption in SOM based on functional group chemistry or putative micro-  
96 domain character”. However, they did not investigate the interaction of nitroxide compounds  
97 containing functional groups such as aniline with SOM.

98 We applied the method of nitroxide spin labeling to investigate the interaction of the functional  
99 amino group to soil humic acid. Signals of nitroxide spin labels, substituted with a functional  
100 group such as aliphatic or aromatic amine, depend on the molecular environment, e.g. polar or  
101 non-polar, and the binding state, e.g. covalently bond. The property of nitroxide radicals to act as

102 good hydrogen bond acceptors [28] does not compromise their use. Moreover, oxidative radical  
103 coupling reaction as a mechanism for covalent binding can be investigated by using a spin  
104 trapping agent [29]. The objectives of our work are to (i) develop the method of nitroxide spin  
105 labeling for the investigation of covalent binding of typical xenobiotic functional groups (here:  
106 aniline) to humic acid as a model for complex soil matrices (proof of concept); (ii) apply the  
107 method for the determination of reaction kinetics of aniline to soil humic acid; (iii) investigate  
108 the influence of phenoloxidase enzyme on the reaction kinetics; and (iv) verify or falsify the  
109 assumption of a radical reaction for the covalent binding of aniline.

## 110 **EXPERIMENTAL SECTION**

111 **Chemicals.** All chemicals were purchased from Sigma-Aldrich (Munich, Germany) if not  
112 otherwise noted. They were analytic grade products and used without further purification.

113 **Humic acid.** Leonardite humic acid (LHA) was purchased from the International Humic  
114 Substances Society (<http://www.humicsubstances.org>). Stock solution of 15 mg/mL was  
115 prepared by dissolution in aqua bidest. and adjusted to pH = 7.0 with 1 M NaOH.

116 **Phenoloxidase.** Extracellular fungal laccase from *Agaricus bisporus* with an activity of 5.6 U  
117 mg<sup>-1</sup> was used without further purification. Stock solutions of 21.4 U/ml were prepared and  
118 stored at 4° C. Aliquots of 10 µL were added to 60 µL of LHA solution and incubated for three  
119 days at room temperature.

120 **Spin labels.** Stock solutions of 3 mM 4-amino-2,2,6,6-Tetramethylpiperidin-1-oxyl (amino-  
121 TEMPO) and 2,5,5-Trimethyl-2-(3-aminophenyl)pyrrolidin-1-yloxy (anilino-NO), synthesized  
122 according to Gadanyi et al. [30], were prepared by dissolution in EDTA-phosphate buffer and  
123 stored at – 80 °C.

124 **ESR Spectroscopy.** ESR spectra were recorded at X-band frequency (9.43 GHz) at room  
125 temperature using a Magnettech Mini Scope MS 200 (Magnettech GmbH, Berlin, Germany).  
126 The microwave power was adjusted to 10 mW and the magnetic field modulation amplitude was  
127 set to 0.2 mT. Samples of 15  $\mu\text{L}$  of 15 mg/mL LHA solution were mixed with 5  $\mu\text{L}$  of 3mM spin  
128 label solution to achieve a final concentration of 750  $\mu\text{M}$  and filled into glass capillaries with an  
129 inner diameter of 0.9 mm (Hirschmann Laborgeräte, Germany). Spectra were recorded in  
130 intervals of four minutes for the first half hour after label addition and afterwards at 1, 2,...5  
131 hours after label addition. Three replicates of each experimental setting were made and fitted  
132 with Origin 7 (OriginLab Corp., USA ) to derive the reaction kinetics. All spectra and graphs  
133 were plotted with Origin 7 and CorelDraw X4 (Corel Inc., Canada).

134 **Radical scavenger.** N-tert-butyl-alpha-phenylnitron (PBN) was used as a spin trap agent. Stock  
135 solution of 300 mM PBN was in turn added to aqueous solutions of LHA, LHA plus laccase,  
136 LHA plus aniline, and finally LHA plus laccase and aniline. Mixtures were made for a final PBN  
137 concentration of 50 mM and a volume of 20  $\mu\text{L}$ . For the laccase settings, LHA and laccase were  
138 mixed in a 6:1 ratio (60  $\mu\text{L}$  LHA + 10  $\mu\text{L}$  laccase) and incubated at room temperature for three  
139 days. A 3 mM aniline stock solution was prepared from anilinium-HCl, adjusted to pH 7, and  
140 mixed with LHA in a 1:4 ratio to obtain a concentration of 750  $\mu\text{M}$ . Fenton's reaction was used  
141 for producing oxygen radicals and testing spin trapping by PBN [31]. For the reaction, 8.5  $\mu\text{L}$  of  
142 200  $\mu\text{M}$  iron sulfate solution and 8.5  $\mu\text{L}$  of 40 mM hydrogen peroxide were mixed. ESR  
143 spectrum was recorded immediately after adding 3.3  $\mu\text{L}$  of 300 mM PBN to this mixture  
144 providing a final concentration of 50 mM.

145 **Spectra simulation.** To analyze the rotational correlation times of the spin labels and the ratios  
146 of free and bound spin labels in the ESR spectra, experimental spectra were fitted using the

147 software Multicomponent774  
148 (<http://www.biochemistry.ucla.edu/biochem/Faculty/Hubbell/software.html>). Spectra were  
149 interpolated using Origin 7, to reduce the number of data points from 4.096 to 512 as required by  
150 Multicomponent774. Simulated spectra were fitted to experimental ESR spectra of amino-  
151 TEMPO in absence and presence of LHA using a model of isotropic Brownian rotational  
152 diffusion. Fitting parameters were the rotational correlation rate, the hyperfine tensor component  
153  $A_{zz}$ , and a Gaussian line width to account for not resolved hyperfine interaction with the methyl  
154 protons. All other parameters were fixed according to typical values for TEMPO derivatives in  
155 aqueous solution ( $g_{xx} = 2.0080$ ,  $g_{yy} = 2.0058$ ,  $g_{zz} = 2.0023$ ,  $A_{xx} = A_{yy} = 0.6$  mT). For fitting of the  
156 spectra of anilino-NO axial symmetry of the reorientational diffusion had to be assumed to  
157 achieve reasonable agreement between simulation and experiment. Thus rotational diffusion was  
158 accounted for by using the two values of the rotational correlation rates parallel and  
159 perpendicular to the symmetry axis,  $R_{\parallel}$  and  $R_{\perp}$ . All other parameters were chosen identical to  
160 those given above. For the simulation of a two component spectrum originating from two  
161 fractions of differently immobilized spin labels a superposition of two spectra was calculated  
162 with two different sets of rotational correlation rates. Fittings were performed of such simulated  
163 two component spectra to the experimental ones with the ratio of the two fractions and the  
164 rotational correlation rates as fitting parameters.

## 165 **RESULTS AND DISCUSSION**

166 **Physical-chemical properties of amino spin labels.** Amino-TEMPO and anilino-NO represent  
167 molecules with amino moieties typical for organic chemicals, which are susceptible to  
168 interaction with humic substances. Among others, the two compounds differ in their lipophilicity  
169 expressed as logarithm of the octanol-water partition coefficient,  $\text{Log } K_{OW}$ , and the acid-base



170 dissociation constant,  $pK_a$ , of the amino group. Measured  $\text{Log } K_{OW}$  of amino-TEMPO are 3.50  
 171 [32] and 3.64 [33] at pH 12 and 0.04 at pH 7 [32].  $pK_a$  values of amino-TEMPO are 8.99 [33]  
 172 and 9.10 [33], respectively. No measured  $\text{Log } K_{OW}$  and  $pK_a$  were available for anilino-NO. With  
 173 KOWWIN of the EPISuite v4.11 package from the U.S. Environmental Protection Agency [34]  
 174 only  $\text{Log } K_{OW}$  values of the hydroxylamine form, i.e. the protonated non-radical N-OH form,  
 175 could be calculated. EPISuite provided values for  $\text{Log } K_{OW}$  of 0.56 for NOH-forms of amino-  
 176 TEMPO and 1.91 of anilino-NO, respectively. We assumed that the difference of 0.52 between  
 177 the measured  $\text{Log } K_{OW}$  of the radical NO-form and the estimated non-radical NOH-form of  
 178 amino-TEMPO represents the fragment of the O-radical and used it to adjust the  $\text{Log } K_{OW}$  value  
 179 of anilino-NO accordingly, which provided a  $\text{Log } K_{OW}$  of 1.39 (Table 1). A  $pK_a$  of the conjugate  
 180 acid of the amino group of anilino-NO of 4.73 (Table 1) was estimated with the SPARC Online  
 181 Calculator [35]. At pH 7, anilino-NO exist in its neutral form, whereas amino-TEMPO is  
 182 protonated at the amino moiety, i.e. it is in the cationic form. This explains the low  $\text{Log } K_{OW}$  of  
 183 amino-TEMPO at pH 7. We thus expect that amino-TEMPO mainly interacts at neutral pH via  
 184 ionic interactions with humic acid. On the other hand, the  $pK_a$  of a non-ionic substance is related  
 185 to its nucleophilic reactivity [15]. Thus, anilino-NO is susceptible to covalent binding due to  
 186 nucleophilic addition reaction with humic acid.

187 **Table 1.** Structure and properties of nitroxide spin labels;

Nitroxide spin label	Amino-TEMPO	Anilino-NO
CAS-No.	14691-88-4	328000-24-4
IUPAC name	4-amino-2,2,6,6-Tetramethylpiperidin-1-oxyl	2,5,5-Trimethyl-2-(3-aminophenyl)pyrrolidin-1-oxyl

Chemical structure		
log K <sub>OW</sub>	3.50 (pH = 12) <sup>1</sup> 0.04 (pH=7) <sup>1</sup> 3.64 ± 0.07 (pH=12) <sup>2</sup>	1.39 <sup>3</sup>
pK <sub>a</sub> of amino group	9.10 ± 0.10 <sup>1</sup> 8.99 ± 0.01 <sup>2</sup>	4.73 <sup>3</sup>

188 <sup>1</sup>) [32]; <sup>2</sup>) [33]; <sup>3</sup>) estimated, see text

189 **LHA incubated with amino-TEMPO.** The relationship between the nitroxide reorientational  
190 motion and the line shape of the continuous wave (cw) spectrum recorded at X-band frequencies  
191 (9 GHz, 0.3 T) has been extensively reviewed [36], thus these properties are summarized in  
192 brief. The term “mobility” is used in the following in a general sense and includes effects due to  
193 the rate, anisotropy and amplitude of the nitroxide reorientation. Weak interaction of a nitroxide  
194 with its micro-environment in solution of low viscosity results in a high degree of mobility. In  
195 this case, the anisotropic components of the hyperfine interaction of the electron with the  
196 nitrogen nuclear spin magnetic moment are averaged out and the spectrum consists of three  
197 equally spaced lines of small width in the order of 0.2 mT. The splitting between the lines is  
198 given by the isotropic component of the hyperfine interaction. In turn, strong interaction of the  
199 nitroxide group with the micro-environment, which restricts unhindered reorientation motion, or  
200 high viscosity of the solvent, are characterized by increased apparent hyperfine splitting and line  
201 widths. The effect of line broadening and corresponding amplitude decrease due to motional  
202 restriction is most pronounced for the high field resonance line. In the limiting case of

203 completely hindered reorientational dynamics the spectrum shows a so-called powder spectrum  
204 line shape [36]. The ESR spectra of amino-TEMPO in aqueous solution and upon incubation  
205 with LHA are shown in Fig. 1.

206 **Fig. 1** ESR spectra recorded at X-band (9.4 GHz) in the B-field region between 333 and 339  
207 mT: amino-TEMPO in aqueous solution (grey continuous line) and upon incubation with LHA  
208 (broken line).

209

210 Three sharp hyperfine lines of nearly equal amplitude reveal unrestricted fast reorientational  
211 motion of amino-TEMPO in aqueous solution. Fitting of simulated ESR spectra to the  
212 experimental ones using the model of isotropic Brownian rotational diffusion yields the value of  
213 the rotational correlation time of  $20 \pm 5$  ps. Upon incubation with LHA the amplitude of the high  
214 field hyperfine absorption signal is significantly reduced (Fig. 1) revealing a decreased mobility  
215 of the nitroxide. Fitting of a simulated spectrum yields a value of the rotational correlation time  
216 of  $95 \pm 10$  ps. Since the viscosity of the used LHA solution is approximately 1.3 times the  
217 viscosity of pure water [37] the observed fivefold increase of the rotational correlation time of  
218 amino-TEMPO must be due to an interaction of the spin label with components of LHA which  
219 restrict its mobility. Possible mechanisms include transient bonding of the amino group via an  
220 ionic interaction to LHA, e.g. cation-exchange sorption<sup>38</sup> or hydrogen bonding of the nitroxide  
221 group to hydrogen donors<sup>39</sup>. Since the experimental spectra do not provide any indication for two  
222 components the weakly bounded and free nitroxide fractions may be in fast equilibrium resulting  
223 in a spectrum with average rotational correlation time.

224 **LHA incubated with anilino-NO.** A different picture evolves for anilino-NO (Fig. 2).  
225 Compared to the EPR spectrum of anilino-NO in aqueous solution (Fig. 2, upper panel) the

226 reduction of the amplitudes of the low field and high field hyperfine absorption signals with  
227 respect to the center line reveal a decreased mobility of anilino-NO in the presence of LHA (Fig.  
228 2, middle panel).

229 **Fig. 2** ESR spectra recorded at X-band (9.4 GHz) in the B-field region between 332 and 340  
230 mT: Anilino-NO in aqueous solution (upper panel) and upon incubation with LHA (measured,  
231 middle panel and simulated, lower panel). The inset in the middle panel highlights the low field  
232 resonance line of the signal of the bound label. For comparison with the experimental spectrum  
233 the simulated spectra for the free and bound components are superimposed in the lower panel.  
234 The concentration of the immobilized component was enhanced by a factor of 2.7 compared to  
235 the experimental case for better visibility.

236  
237 Reasonable fitting of simulated spectra to the experimental ones required a model of axial  
238 symmetry of the rotational diffusion with the symmetry axis being parallel to the nitroxide y-  
239 axis. From the reorientational rates parallel and perpendicular to this axis,  $R_{\parallel}$  and  $R_{\perp}$ , an  
240 effective reorientational correlation time

$$241 \quad \tau = \frac{1}{6\sqrt{R_{\perp}R_{\parallel}}} \quad (1)$$

242 was calculated. For anilino-NO in aqueous solution and in the presence of LHA we determined  
243 correlation times of  $50 \pm 23$  ps and  $219 \pm 53$  ps, respectively. Similar to the finding with amino-  
244 TEMPO the increase of the rotational correlation time by a factor of four cannot be explained by  
245 the increase of the viscosity of the solution upon incubation with LHA. Thus, we conclude that a  
246 transient weak interaction of anilino-NO with components of LHA, e.g., hydrogen bonding to the  
247 nitroxide group or hydrophobic interaction, is responsible for the decrease of reorientational  
248 motion. Axial symmetry of rotational diffusion with the symmetry axis parallel to the y-axis of

249 the nitroxide can be readily explained by the shape of the molecule with its longest axis oriented  
250 nearly parallel to the nitroxide y-axis (Fig. 3).

251 **Fig. 3** Structure of anilino-NO with orthogonal coordinate system

252 In addition to this weakly immobilized spin label, a broad spectral component is present which  
253 indicates strongly immobilized anilino-NO. This component is most clearly resolved in the low  
254 and high field regions of the spectrum (see Fig. 2, insert for the low field region). Thus, a  
255 fraction of anilino-NO is immobilized due to strong bonding to LHA, which restricts the  
256 reorientational dynamics of the nitroxide moiety. A simulated spectrum with two components of  
257 weakly and strongly immobilized spin labels is shown in Fig. 2, lower panel, with the component  
258 for the strongly immobilized spin label enlarged compared to the experiment spectrum for  
259 clarity. Reorientational correlation times of weakly and strongly immobilized anilino-NO  
260 determined from fittings of simulated two component spectra to the experimental ones yielded  
261  $219 \pm 53$  ps and  $6.2 \pm 0.9$  ns, respectively.

262 The ESR spectrum of LHA incubated with anilino-NO leads to the conclusion that humic acids  
263 play a significant role in binding of aromatic amino-groups of xenobiotics. It is known, that  
264 oxidizing catalyst, e.g. phenoloxidase enzymes or metal oxides, enhance the covalent binding of  
265 functional aniline group to humic acids [20, 22]. Therefore, we additionally used laccase as an  
266 oxidizing enzyme to investigate the activating effect on the reaction kinetics (see below).

267 **Spin number ratio.** For sake of simplicity the weakly and strongly immobilized spin labels will  
268 be labeled “free” and “bound” in the following. The ratio of the spin number of the bound to that  
269 of the free species,  $N_{\text{bound}}/N_{\text{free}}$ , is used for the determination of the reaction kinetics. It is

270 calculated from the corresponding ratio of the peak height (amplitude) of the low field resonance  
271 line of the signal of the bound to that of the free, unbound label according to:

$$272 \quad \frac{N_{bound}}{N_{free}} = 45.9 \cdot \frac{amplitude_{bound}}{amplitude_{free}} \quad (2)$$

273 The factor 45.9, which relates the ratio of spin numbers to that of spectral amplitudes, was  
274 determined from the simulated spectrum shown in Fig. 2, lower panel. Here, the ratio of the spin  
275 numbers was calculated from the ratio of the double integrals of the spectra of the two  
276 components, the ratio of the amplitudes was determined from their values at 330.0 and 334.0  
277 mT.

278 **Kinetic studies.** Spectra were recorded immediately after mixing of the spin labelled molecules  
279 with LHA and repeated every few minutes. Intervals were increased with reaction time. Fig. 4  
280 shows the peak of the strongly bound anilino-NO within the first five hours.

281

282 **Fig. 4** ESR signal of the bound species of anilino-NO incubated with LHA

283

284 The spin number ratio is plotted against time in Fig. 5. The narrow variance of the three  
285 replicates demonstrates complete mixing and the precision and reproducibility of the  
286 measurements. Note that the right amplitude axis belongs to the data recorded without laccase.  
287 The first data point, measured after a few minutes mixing time, was set to zero although the  
288 signal of the bound species was already visible. This was done for all settings because the  
289 starting point of the reaction is undefined. A mono-exponential (2) and a bi-exponential model  
290 (3) were tested for fitting the experimental data:

291 
$$f(t) = a_1 \cdot (1 - e^{-b_1 t}) \quad (3)$$

292 
$$f(t) = a_1 \cdot (1 - e^{-b_1 t}) + a_2 \cdot (1 - e^{-b_2 t}) \quad (4)$$

293 The coefficients  $a_i$  denote the relative amount of anilino-NO reacting with LHA and  $b_i$  are the  
294 pseudo-first-order reaction rate constants. Table 2 shows the fitted model parameters for both  
295 models. The mono-exponential model reveals values of  $0.18 \pm 0.004$  for  $a_1$  and  $0.03 \pm 0.002$   
296  $\text{min}^{-1}$  for  $b_1$ , corresponding to a half-time of 24 min. However, a better fit was achieved with  
297 two parallel first-order reactions. The two reactions have pseudo-first-order rate constants  $b_1$  and  
298  $b_2$  of  $0.01 \pm 0.001$  and  $0.16 \pm 0.017 \text{ min}^{-1}$ , which corresponds to half-times of 69.3 and 4.3 min,  
299 respectively. The relative amount of the reacting species  $a_1$  is  $0.14 \pm 0.002$  and thus 2.8 times  
300 greater than  $a_2$ , which is  $0.05 \pm 0.003$ . Thus, the very fast reaction determines the overall  
301 increase of the bound anilino-NO label only at the very beginning. Colon et al. 2002<sup>15</sup>  
302 determined kinetic data for the reaction of ortho-, meta- and para-substituted anilines with  
303 sediment and found two pseudo-first-order rate constants depending on the substitution pattern.  
304 Corresponding half-times were around 20 h and 500 h and thus larger than those found with the  
305 spin labeling method. After  $t = 4$  h incubation time of aniline in a pond sediment, Weber et al.  
306 2001<sup>8</sup> found sorbed aniline fractions of 0.18 and 0.16 at  $\text{pH} = 6.82$  and  $7.37$ , respectively. They  
307 attributed them to rapid covalent binding of the neutral form of aniline but could not determine  
308 the rate constants. They observed a longer term sorption rate ( $t > 4$  h) with pseudo-first-order rate  
309 constants of around  $0.005 \text{ h}^{-1}$ , which correspond to the findings of Colon et al. [15]. Hennecke  
310 (personal communication) investigated the aerobic and anaerobic transformation of aniline in the  
311 water-sediment simulation system according the OECD Test Guideline 308 [40] and found very  
312 rapid formation of NER in sediment with high organic carbon content up to 62 % of the applied  
313 radioactivity immediately after adding. However, they could not determine the rate constant of  
314 the very rapid NER formation.

315

316 **Fig. 5** Plot of the spin number ratio versus time of the bound species of anilino-NO incubated  
 317 with LHA without (black, right y-axis) and upon incubation with (red, left y-axis) laccase; bold  
 318 and dashed lines are fitted curves according to the bi- and mono-exponential kinetic model.

319

320

321 **Table 2** Fitted model parameters for mono- and bi-exponential reaction kinetics of  
 322 anilino-NO with LHA and with LHA incubated with laccase.

Setting	Relative amount of fast reacting species $a_1$	Rate constant fast reaction $b_1$ [ $\text{min}^{-1}$ ]	Relative amount of very fast reacting species $a_2$	Rate constant of very fast reaction $b_2$ [ $\text{min}^{-1}$ ]	Coefficient of determination, $r^2$
LHA (bi-exp)	$0.14 \pm 0.002$	$0.01 \pm 0.001$	$0.05 \pm 0.003$	$0.16 \pm 0.017$	0.999
LHA (mono-exp)	$0.18 \pm 0.004$	$0.03 \pm 0.002$	-	-	0.988
LHA+ Laccase (bi-exp)	$1.07 \pm 0.015$	$0.01 \pm 0.001$	$0.06 \pm 0.016$	$0.27 \pm 0.29$	0.998
LHA + Laccase (mono-exp)	$1.09 \pm 0.022$	$0.01 \pm 0.001$	-	-	0.999

323

324 Laccase is known to catalyze the formation of covalent bonds by oxidizing unreactive  
 325 hydroquinone moieties in humic substances to electrophilic quinone moieties [6, 8, 23]. We thus  
 326 incubated LHA with extracellular fungal laccase from *Agaricus bisporus* for three days at room  
 327 temperature and mixed it with anilino-NO. Fig. 4-5 shows the spin number ratio plotted against  
 328 time. Note that the left y-axis belongs to the setting with laccase. A larger amount of anilino-NO  
 329 reacting with LHA was observed than in the experiments without laccase. Again, a mono- and  
 330 bi-exponential model was used for fitting. Obviously, both models give almost the same data fit.



331 The kinetic model parameters  $a_1$  and  $b_1$  are thus also almost identical, i.e.  $1.09 \pm 0.022$  and  $0.01$   
332  $\pm 0.001 \text{ min}^{-1}$  for the mono-exponential and  $1.07 \pm 0.015$  and  $0.01 \pm 0.001 \text{ min}^{-1}$  for the bi-  
333 exponential model, respectively (Table 2). The very fast reaction with  $b_2 = 0.27 \pm 0.29 \text{ min}^{-1}$  has  
334 a neglecting influence on the covalent binding of anilino-NO to LHA due to the low value of  $a_2$   
335  $= 0.06 \pm 0.016$ , which is 17.8 lower than  $a_1$ . The treatment with laccase has obviously activated  
336 only the slower reacting LHA sites. The rate constants for the reaction are identical for the  
337 settings with and without laccase, whereas the relative amount of reacting species is considerably  
338 enhanced from 0.14 to 1.07, which is factor of 7.6. This finding is in line with the observations  
339 of other authors [10, 21, 23], who showed the increase of reactive sites of humic substances  
340 mediated by the phenoloxidase enzyme laccase. We conclude from our kinetic study with laccase  
341 that the broadened signal of anilino-NO can be attributed to covalent binding to LHA,  
342 presumably a nucleophilic addition to quinones or other carbonyl moieties.

343 **Radical coupling reaction.** Radical reactions involving free radical intermediates and  
344 semiquinone radicals have also been proposed as covalent binding mechanism [2]. We thus  
345 added the spin trap agent PBN, which displays a characteristic ESR spectrum if free radicals are  
346 present in a sample. For comparison, Fenton's reaction was used to produce free radicals, which  
347 react with PBN to stable spin adducts. Fig. 6 shows ESR spectra of PBN incubated with LHA  
348 and  $750 \mu\text{M}$  aniline (bottom), with laccase and  $750 \mu\text{M}$  aniline (middle), and with Fenton's  
349 reagent (top). ESR spectra of LHA without and with laccase show the unchanged broad signal of  
350 the organic radicals, which are typical for humic acids [41] but no additional peaks from free  
351 radicals or spin adducts with PBN. If free radicals would have been produced in the LHA  
352 experiments, i.e. radicals intermediates or/and radical semiquinones, similar spectra as with  
353 Fenton's reagent would have been recorded. From the absence of the characteristic PBN spin

354 adduct spectrum we conclude that oxidative radical coupling can be excluded as a mechanism of  
355 the covalent binding of anilino-NO to LHA, even in the presence of laccase.

356

357 **Fig. 6** Plot of experimental spectra of LHA with aniline (bottom), aniline and laccase (middle)  
358 and Fenton's reaction (top) in presence of 50 mM PBN. Top spectrum displays characteristic  
359 PBN spectral lines produced by radical reaction. Ordinate axis of top spectrum is enhanced by  
360 1.8 relative to the other two spectra.

361

## 362 **CONCLUSION**

363 Our ESR experiments with labelled aniline as a model compound have shown in a proof-of-  
364 concept approach that the method can be used to identify strong binding of aromatic amines and  
365 determine its reaction kinetics to humic acid, an important soil constituent. Derivatives of  
366 nitroxide radicals are stable enough to study the interaction of specific functional groups to  
367 isolated humic substances as model compounds. We conclude from the spectral differences of  
368 the two amine substituted nitroxide radicals that the aromatic amino group covalently binds to  
369 humic substances at neutral pH, while aliphatic amines presumably interact via cation exchange  
370 or hydrogen bonding of the nitroxide group to hydrogen donors of LHA. Covalent binding of  
371 labelled aniline was evidenced by adding laccase. Oxidative radical coupling could be excluded  
372 by using the spin trapping agent PBN.

373 Our experiments demonstrated the suitability of nitroxide labels to investigate the interaction of  
374 xenobiotic chemicals with humic acids. In particular, the fast reaction of aniline with HA could  
375 not yet be revealed with other methods so far. It could explain the rapid loss of the extractability  
376 of sulfonamides after application to natural soil [17 – 19]. Humic acids have a wide distribution  
377 of potential reaction sites, which might be activated by treatment with laccase or other oxidizing

378 enzymes. The fast reaction of aniline with LHA observed with the nitroxide spin label might be a  
379 first step in a series of subsequent binding processes [23]. Covalent binding can unambiguously  
380 distinguished from other sorption processes such as sequestration, which would less restrict  
381 mobility of the spin labelled molecule. The specificity of the interaction process coupled with the  
382 sensitivity of the spin label signals make the method also suitable for more complex systems like  
383 soil and sediment. Recently, nitroxide spin probing experiments with natural soil [42] have  
384 demonstrated the potential of the method for investigating the interaction of xenobiotic  
385 functional groups with complex soil systems.

386

## 387 **AUTHOR INFORMATION**

### 388 **Corresponding Author**

389 \*Phone: 0049-541 969 2576; fax: 0049-541 969 2599; e-mail: matthies@uos.de

### 390 **Notes**

391 The authors declare no competing financial interest.

## 392 **ACKNOWLEDGEMENTS**

393 We kindly acknowledge the lab-assistance of Elena Bondarenko. Support of the Hungarian  
394 National Research Fund OTKA [K104956](#) is greatly acknowledged.

395

396

397

398 REFERENCES

- 399 (1) M. Kästner, K. M. Nowak, A. Miltner, S. Trapp, A. Schäffer, *Crit. Rev. Environ. Sci.*  
400 *Technol.* 44, 2107 (2013)
- 401 (2) N. Senesi, *Sci. Tot. Environ.*, 123/124, 63 (1992)
- 402 (3) F. Führ, H. Ophoff, *Pesticide Residues in Soil*, (Wiley-VCH, Weinheim, 1998)
- 403 (4) B. Gevaio, K.T. Semple, K.C. Jones, *Environ. Pollut.* 108, 3 (2000)
- 404 (5) E. Barriuso, P. Benoit, I. G. Dubus, *Environ. Sci. Technol.* 42, 1845 (2008)
- 405 (6) G. E. Parris, *Environ. Sci. Technol.* 14, 1099 (1980)
- 406 (7) J.-M. Bollag, C. Myers, *Sci. Tot. Environ.* 117-118, 357 (1992)
- 407 (8) E. J. Weber, D. Colón, G. L. Baughman, *Environ. Sci. Technol.* 35, 2470 (2001)
- 408 (9) C. Achtnicht, E. Fernandes, J.-M. Bollag, H.-J. Knackmuss, H. Lenke, *Environ. Sci.*  
409 *Technol.* 33, 4448 (1999)
- 410 (10) G. Dawel, M. Kästner, J. Michels, W. Poppitz, W. Günther, W. Fritsche, *Appl. Environ.*  
411 *Microbiol.* 63, 2560 (1997)
- 412 (11) K. A. Thorn, K.R. Kennedy, *Environ. Sci. Technol.* 36, 3787 (2002)
- 413 (12) E. J. Weber, D. L. Spidle, K. A. Thorn, *Environ. Sci. Technol.* 30, 2755 (1996)
- 414 (13) K. A. Thorn, P. J. Pettigrew, W. S. Goldenberg, *Environ. Sci. Technol.* 30, 2764 (1996)
- 415 (14) H. Li, L. S. Lee, *Environ. Sci. Technol.* 33, 1864 (1999)
- 416 (15) D. Colón, E. J. Weber, G. L. Baughman, *Environ. Sci. Technol.* 36, 2443 (2002)
- 417 (16) J.-M. Bollaq, *Environ. Sci. Technol.* 26, 1876 (1992)
- 418 (17) T. Müller, I. Rosendahl, A. Focks, J. Siemens, J. Klasmeier, M. Matthies, *Environ.*  
419 *Pollut.* 172, 180 (2013)
- 420 (18) M. Förster, V. Laabs, M. Lamshöft, J. Groeneweg, M. Krauss, M. Kaupenjohann, W.  
421 *Amelung*, *Environ. Sci. Technol.* 43, 1824 (2009)
- 422 (19) A. Gulkowska, B. Thalmann, J. Hollender, M. Krauss, *Chemosphere* 107, 366 (2014)
- 423 (20) H. M. Bialk, A. J. Simpson, J. A. Pedersen, *Environ. Sci. Technol.* 39, 4463 (2005)
- 424 (21) H. M. Bialk, C. Hedman, A. Castillo, J. A. Pedersen, *Environ. Sci. Technol.* 15, 3593  
425 (2007)
- 426 (22) H. M. Bialk, J. A. Pedersen, *Environ. Sci. Technol.* 42, 106 (2008)
- 427 (23) A. Gulkowska, M. Sander, J. Hollender, M. Krauss, *Environ. Sci. Technol.* 47, 2102  
428 (2013)
- 429 (24) J. P. Klare, H.-J. Steinhoff, *Spin Labeling EPR. Photosynth. Res.* 102, 377 (2009)
- 430 (25) J. P. Klare, H.-J. Steinhoff, in *Structural information from spin-labels and intrinsic*  
431 *paramagnetic centres in the biosciences*, ed. by C. R. Timmel, J. R. Harmer (Book Series:  
432 *Structure and Bonding* 152, Springer, Berlin, 2013), pp. 205-248

- 433 (26) A. D. Steen, C. Arnosti, L. Ness, N. V. Blough, *Mar. Chem.* 101, 266 (2006)
- 434 (27) C. Lattao, X. Cao, Y. Li, J. Mao, K. Schmidt-Rohr, M.A. Chapell, L. F. Miller, A. L.  
435 dela Cruz, J. J. Pignatello, *Environ. Sci. Technol.* 46, 12814 (2012)
- 436 (28) P. Franchi, M. Lucarini, P. Pedrielli, G. F. Pedulli, *Chem. Phys. Chem.* 3, 789 (2002)
- 437 (29) G. R. Buettner, *Free Radic. Biol. Med.* 3, 259 (1987)
- 438 (30) S. Gadányi, T. Kálai, J. Jekő, Z. Berente, K. Hideg, *Synthesis* 32, 2039 (2000)
- 439 (31) K. Stolze, N. Udilova, H. Nohl, *Acta Biochim. Polon.* 47, 923 (2000)
- 440 (32) J. Fuchs, W. H. Nitschmann, L. Packer, O. H. Hankovszky, *Free Rad. Res. Comms.* 10,  
441 315 (1990)
- 442 (33) A. P. Todd, R. J. Mehlhorn, R. I. Macey, *J. Membrane Biol.* 109, 41 (1989)
- 443 (34) Estimation Programs Interface Suite™ for Microsoft® Windows, v 4.11 (United  
444 States Environmental Protection Agency, Washington, 2012), [http://www.epa.gov/tsca-](http://www.epa.gov/tsca-screening-tools/epi-suitetm-estimation-program-interface)  
445 [screening-tools/epi-suitetm-estimation-program-interface](http://www.epa.gov/tsca-screening-tools/epi-suitetm-estimation-program-interface).
- 446 (35) SPARC on-line calculator: <http://archemcalc.com/sparc-web/calc> (2015)
- 447 (36) L. J. Berliner, Ed. *Spin Labeling: Theory and Applications*, (Academic Press, New York,  
448 1976)
- 449 (37) M. Kawahigashi, H. Sumida, K. Yamamoto, *J. Coll. Interf. Sci.* 284, 463 (2005)
- 450 (38) S. T. J. Droge, K.-U. Goss, *Environ. Sci. Technol.* 47, 798 (2013)
- 451 (39) L. Urban, H.-J. Steinhoff, *Mol. Phys.* 111, 2873 (2013)
- 452 (40) OECD Guideline for the Testing of Chemicals no. 308: Aerobic and Anaerobic  
453 Transformation in Aquatic Sediment Systems (Organisation of Economic Cooperation and  
454 Development, Paris, 2002)
- 455 (41) A. Jezierski, F. Czechowski, M. Jerzykiewicz, Y. Chen, J. Drozd, *Spectrochim. Acta A*  
456 56, 379 (2000)
- 457 (42) M. Matthies, M. Theiling, K. Hideg, H.-J. Steinhoff, SETAC Europe Conference,  
458 Barcelona (2015), p. 27
- 459

460

461 **Figure captions**

462

463 **Fig. 1** ESR spectra recorded at X-band (9.4 GHz) in the B-field region between 333 and 339  
464 mT: amino-TEMPO in aqueous solution (grey continuous line) and upon incubation with LHA  
465 (broken line).

466 **Fig. 2** ESR spectra recorded at X-band (9.4 GHz) in the B-field region between 330 and 340  
467 mT: Anilino-NO in aqueous solution (upper panel) and upon incubation with LHA (measured,  
468 middle panel and simulated, lower panel). The inset in the middle panel highlights the low field  
469 resonance line of the signal of the bound label. For comparison with the experimental spectrum  
470 the simulated spectra for the free and bound components are superimposed in the lower panel.  
471 The concentration of the immobilized component was enhanced by a factor of 2.7 compared to  
472 the experimental case for better visibility.

473 **Fig. 3** Structure of anilino-NO with orthogonal coordinate system

474 **Fig. 4** ESR signal of the bound species of anilino-NO incubated with LHA

475 **Fig. 5** Plot of the spin number ratio versus time of the bound species of anilino-NO incubated  
476 with LHA without (black, right y-axis) and upon incubation with (red, left y-axis) laccase; bold  
477 and dashed lines are fitted curves according to the bi- and mono-exponential kinetic model.

478 **Fig. 6** Plot of experimental spectra of LHA with aniline (bottom), aniline and laccase (middle)  
479 and Fenton's reaction (top) in presence of 50 mM PBN. Top spectrum displays characteristic  
480 PBN spectral lines produced by radical reaction. Ordinate axis of top spectrum is enhanced by  
481 1.8 relative to the other two spectra.

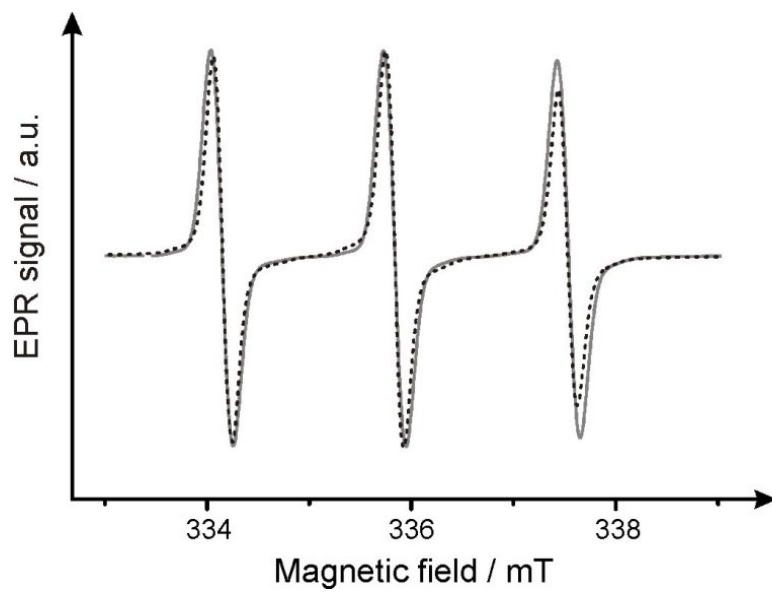
482

483

484 Fig. 1

485

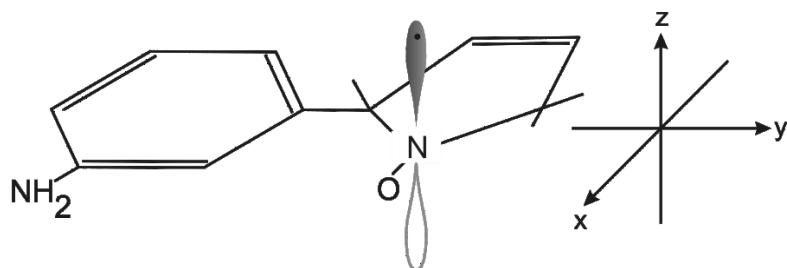
486



487

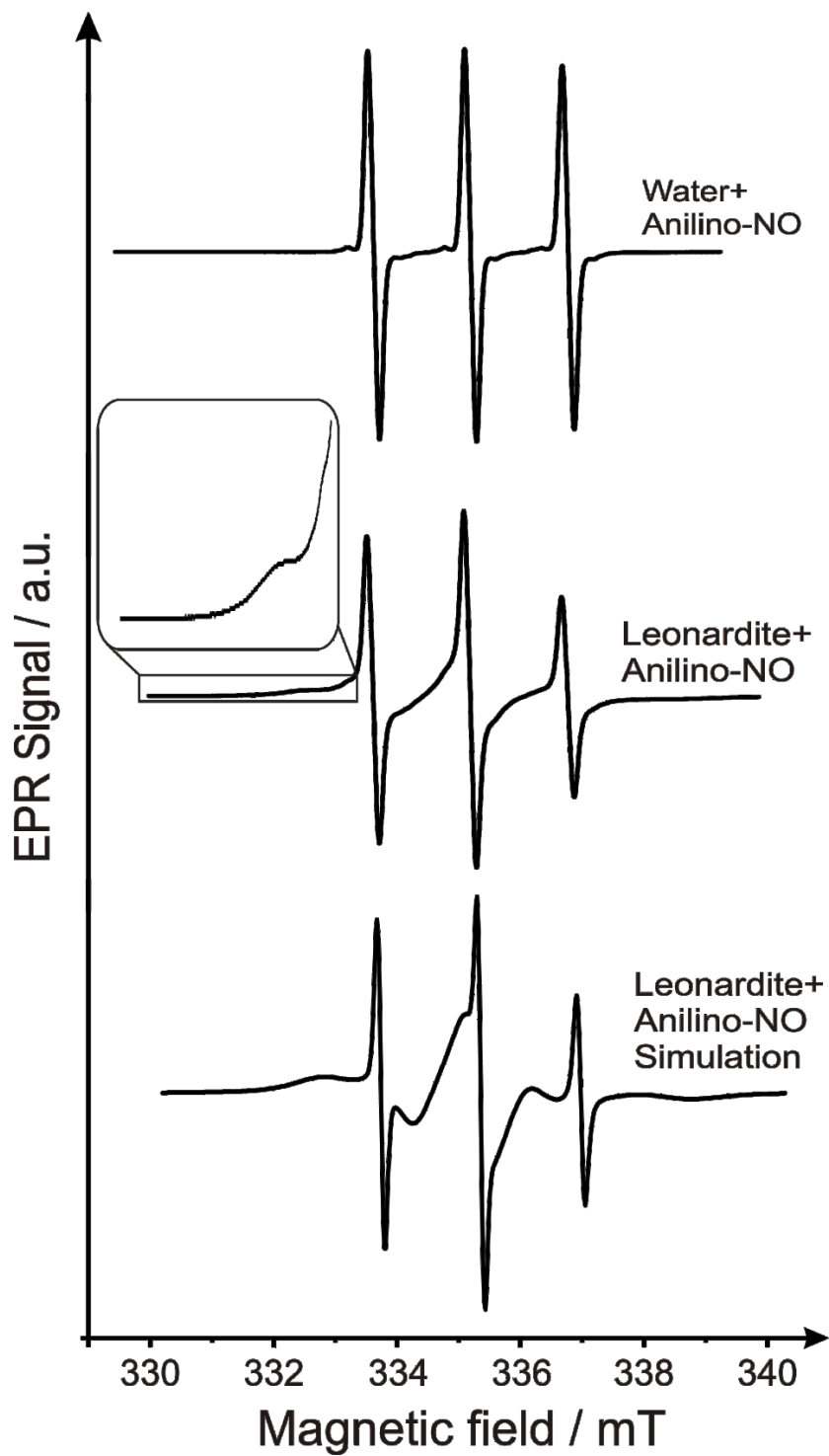
488

489  
490 Fig. 2  
491  
492  
493  
494

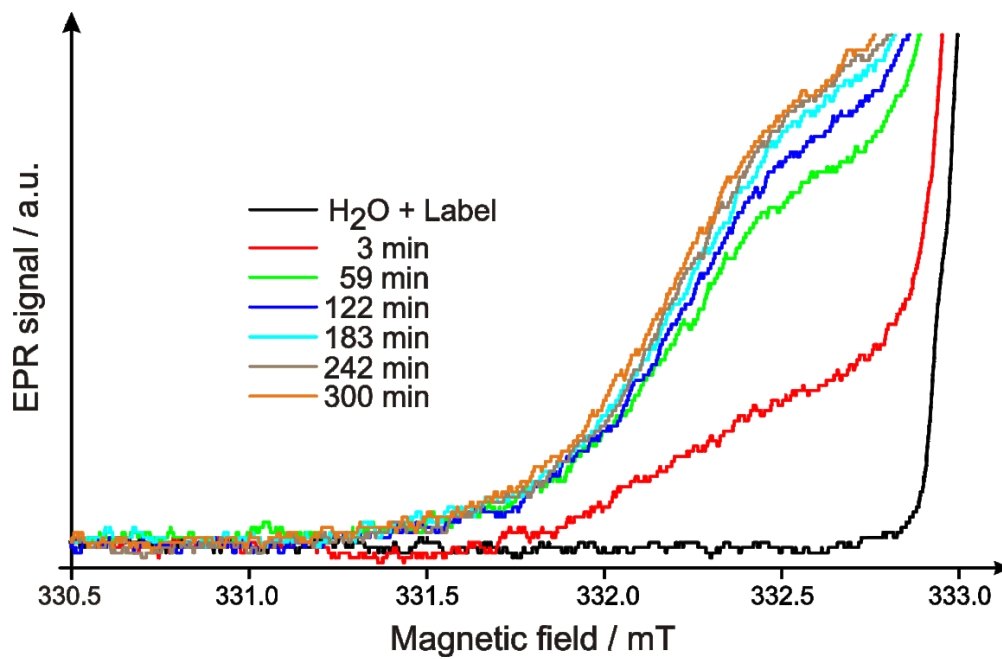


495  
496  
497



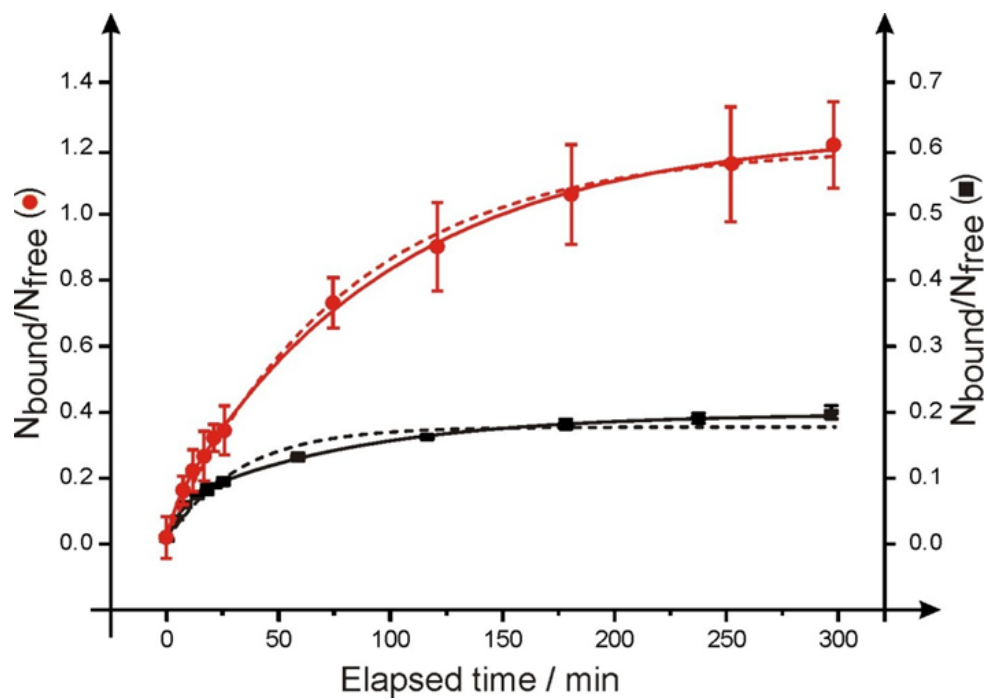


503  
504 Fig. 4  
505



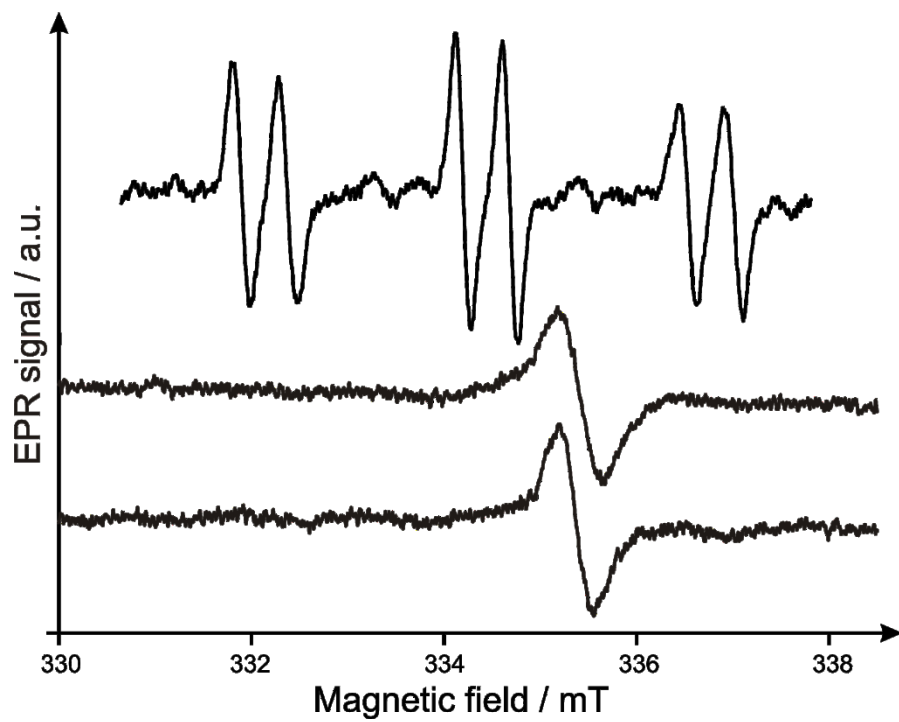
506  
507

508  
509 Fig. 5  
510  
511



512  
513

514  
515 Fig. 6  
516



517  
518